Following Jahn-Teller distortions in fulleride salts by optical spectroscopy

G. Klupp and K. Kamarás

Abstract C_{60} salts represent perfect model systems for the Jahn-Teller effect, in particular for the interplay between the molecular dynamics and the distorting crystal field. In this paper, after a brief introduction to the theoretical background, we review experimental results on salts with fulleride anions containing different charge states in the solid state. Mid-infrared (MIR) and near infrared (NIR) spectroscopic measurements and their conclusions are reported in detail, while the results obtained by nuclear magnetic resonance (NMR), electron spin resonance (ESR) and X-ray diffraction are briefly summarized. The following questions are addressed: Are fulleride ions distorted in various solids? Is the distortion dominated by the molecular Jahn-Teller effect or by the potential field of the environment? What is the shape of the distortion? Is the distortion static or dynamic, is there a pseudorotation, are there transitions between static and dynamic JT states? How do these effects manifest themselves in vibrational and electronic excitations? The experimental difficulties one has to face when studying Jahn-Teller distortions in solids are also discussed. These limitations originate not only in the performance of the spectroscopic methods used, but also in the chemistry of some of the compounds, which can lead to segregation and polymerization.

1 Introduction to the theory of the Jahn-Teller effect in fulleride ions

The neutral C_{60} molecule possesses the highest symmetry point group found in nature, the icosahedral I_h group (see Fig. 1). This high symmetry leads to degeneracies of both the electronic and vibrational energy levels. Its HOMO (highest occupied molecular orbital), LUMO (lowest unoccupied molecular orbital) and LUMO+1 (next lowest unoccupied molecular orbital) belong to the h_u, t_{1u} and t_{1g} represen-

Research Institute for Solid State Physics and Optics, Hungarian Academy of Sciences, Budapest, Hungary, e-mail: klupp@szfki.hu, kamaras@szfki.hu

tation, respectively [1]. The LUMO can be partially or completely filled with electrons upon reacting C_{60} with suitable electron donors, e.g. alkali metals. This way a C_{60}^{n-} ($n < 6$) molecular ion with degenerate electronic states is formed, which is subject to Jahn-Teller distortion. The t orbital can couple to vibrational modes of H_g and A_g symmetry [2]. Since the A_g vibrations do not change the symmetry of the molecule, we will only consider H_g vibrations in the following. As we will see below, the fulleride ions have a spherical APES (adiabatic potential energy surface) in the first approximation. Thus the notation commonly used for the fulleride ions as Jahn-Teller systems is $p^n \otimes H$ in analogy with the p^n electron configuration of atoms [3].

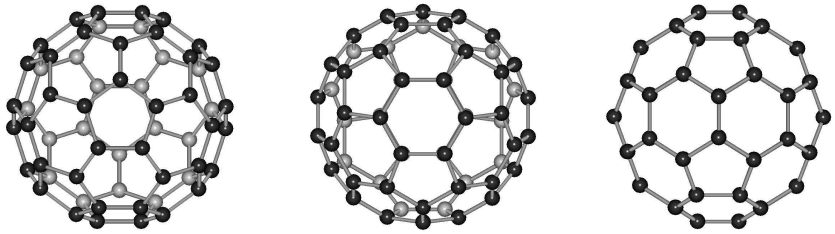

Fig. 1 The icosahedral symmetry of the C_{60} molecule. The atoms above the plane of the paper are marked black, those under it grey. In the left figure one of the C_5 and S_{10} axes is perpendicular to the plane of the paper. This is the axis along which the C_{60}^{-}, the C_{60}^{2-} and the C_{60}^{4-} molecules are elongated or compressed by a D_{5d} distortion. In the figure in the middle, one of the C_3 and S_6 axes is perpendicular to the plane of the paper. This is the axis along which the above molecules are distorted in a D_{3d} symmetry. In the right figure a C_2 axis is perpendicular to the plane of the paper, another C_2 axis is horizontal, and the third one is vertical. In this figure one of the mirror planes of the molecule coincides with the plane of the paper, the other two are perpendicular to it and to each other. [4] Copyright (2006) by the American Physical Society.

The Hamiltonian of the $p^n \otimes H$ system for linear coupling can be written as [3]:

$$\hat{\mathcal{H}} = -\frac{1}{2}\sum_{i=1}^{5}\frac{\partial^2}{\partial Q_i^2} + \frac{1}{2}\sum_{i=1}^{5} Q_i^2 + \hat{M}(Q_i), \tag{1}$$

where $\hat{M}(Q_i)$ is the vibronic interaction energy and Q_i are the five normal coordinates spanning a five dimensional space containing the APES. The different energy terms are in $\hbar\omega$ units, where ω is the frequency of the coupled vibration.

After a change of variables in the potential energy $\hat{V}$, it becomes apparent that the APES has a minimum not only at a single point, but in a three dimensional spherical subspace of the five dimensional Q space [3, 5]. The smallest eigenvalue of the M matrix is $-\eta k Q$, where k is the vibronic coupling constant and η is a constant depending on the charge state of the fulleride ion [5]. Substituting this into $\hat{V}$ we get

$$\hat{V} = \frac{1}{2}Q^2 - \eta k Q; \tag{2}$$

and a minimum at $Q = \eta k$. The result is the same if we take into account all of the 8 H_g modes of C_{60}^{n-} [6]. Thus the minimum of the APES is a three dimensional spherical surface with a radius of ηk [3, 7].

If a molecule with I_h symmetry is distorted by the JT effect in the direction of an H_g vibration, its point group will become D_{2h}, D_{3d} or D_{5d} [5, 8]. The distortion corresponding to the minimum of the APES is a prolate in the $p \otimes H$ and the $p^2 \otimes H$ system and an oblate in the $p^4 \otimes H$ and the $p^5 \otimes H$ system [7]. The different points of the APES correspond to different directions of the main axis of these spheroids. As all points corresponding to the minimum of the APES are equivalent, all distortions corresponding to these points are equally probable. This leads to a continuously wandering main distortion axis: the molecule performs pseudorotation [3, 7]. In the course of the pseudorotation the point group of the molecule changes, but it remains icosahedral on the average.

For the $p^3 \otimes H$ system one possible shape of the distortion is depicted in Fig. 2.b. It can be seen that the distortion is not symmetric about any axis in this case [7]. Although the shape is not the same as in the other anions, this molecule will also perform pseudorotation.

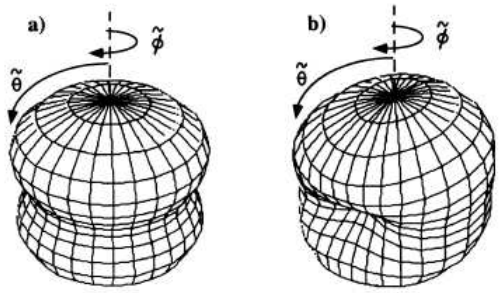

Fig. 2 One possible shape of the Jahn-Teller distortion of C_{60}^{n-} a) for n = 1, 2, 4, 5 and b) for n = 3. [7] Copyright (1994) by the American Physical Society.

If nonlinear terms of the vibronic coupling are also taken into account or we allow for anharmonic interatomic forces, the spherical symmetry of the minima of the APES will be lost [5, 9]. The distortions corresponding to the new minima on the APES have to bear the highest possible symmetry [9]. Depending on the parameters, this scenario can be achieved if the lowest energy configurations belong to the D_{3d}, D_{5d}, or D_{2h} configurations [5, 6, 10].

The isolated C_{60}^{n-} molecule can be distorted into six different directions with D_{5d} symmetry and ten directions with D_{3d} symmetry. In the isolated molecule the distortions belonging to the same point group but pointing in different directions

have the same energy [6]. The barrier between these distortions is small, so the molecule can move from one distortion to the other via pseudorotation [11, 12].

Relatively few theoretical works have attempted to determine the exact distortion where the APES of the isolated molecule has minima. An early Hartree-Fock calculation by Koga and Morokuma on C_{60}^{-} found no significant energy difference between D_{2h}, D_{3d} and D_{5d} geometries [13], but resulted in the correct prolate shape. Green et al. performed DFT (density functional theory) calculations on isolated C_{60}^{n-} anions [14]. They also found very small energy differences between different distortions in most of the anions. The lowest energy configuration was D_{3d} in the case of C_{60}^{-}. The triplet and singlet state of C_{60}^{2-} were also very close in energy, with D_{3d} and D_{2h} geometry, respectively. The C_{60}^{3-} had an icosahedral quartet ground state. The C_{60}^{4-} ion and the C_{60}^{5-} ion are the electron-hole analogues of the C_{60}^{2-} and the C_{60}^{-} ions concerning their frontier MOs. Despite this fact, the calculation led to a D_{5d} configuration of the triplet C_{60}^{4-}.

In real fulleride salts we also have to consider the potential field generated by the environment in a solid. In alkali fullerides containing cations larger than Na^{+}, the dominating interaction is the repulsion between the cation and the anion arising from wave function overlap, i.e. the steric crowding [15]. This potential field generated by the alkali metal ions is the crystal field (a strain) which can lower the potential energy of a specific distortion. If the barrier to other minima on the APES of the molecule is high, a static distortion appears [3]. If the barrier is lower than the thermal energy, the distortion is still dynamic.

Going from the molecular picture to that of collective properties in a solid means adding translational symmetry to the point group symmetry. The theoretical description does this by introducing a phase of the distortion throughout the material, which is determined by the spatial variation of the variously distorted molecules. If, as is usual in a classical crystal, the phase of the distortion shows the translational symmetry of the solid, the so-called cooperative Jahn-Teller effect appears where the shape of one molecule and the space group determines the shape of all the others. If the distortions are not correlated, however, the phase is random and the situation is not different from that of isolated molecules. This is the dynamical Jahn-Teller effect where the distortions cannot be detected but the solid-state consequences still appear in the electronic structure [16].

Thus in fulleride solids, depending on the interplay of several parameters, multiple phases are possible and phase transitions can occur when varying the cation size or the temperature or pressure. Dunn [11] has investigated these effects in detail for the cooperative Jahn-Teller effect in solids and gave a general description for icosahedral systems.

Fabrizio and Tosatti introduced the idea of the Mott-Jahn-Teller insulator and performed a model calculation for an $E \bigotimes e$ system. Dunn [11, 17] extended this model to the $p^n \bigotimes h$ system for fullerenes and determined the properties of various cooperative JT distorted phases.

2 Experimental methods used in the detection of Jahn-Teller distortions

In this section, we briefly summarize the principles of the measurements which can be applied to detect the consequences of the JT effect on physical properties. We will start with a short summary of the most widely applied methods, and then give a detailed description on vibrational and optical spectroscopy of fullerene solids, where to our knowledge no comprehensive review exists. On other topics, excellent overviews have been written, e.g. by Reed and Bolskar [18] on structural and spectroscopic (near infrared, nuclear magnetic resonance and electron spin resonance) investigations on discrete fulleride anions, by Brouet et al. [19] on collective magnetic properties detected by nuclear magnetic resonance spectroscopy, and by Arcon and Blinc [20] on the detection of pseudorotational dynamics by nuclear resonance.

We have to state right away that the experimentalist trying to determine the consequences of the JT effect in fullerides has no easy task. Part of the difficulties stem from the material and part from the complicated and intertwined phenomena which occur in most systems containing fullerene balls. The first step is to prepare the appropriate materials in homogeneous and stable form; the second, once the measurements are done, to isolate the effects of Jahn-Teller origin from the vast amount of exotic phenomena caused by the environment or physical conditions as temperature and pressure. The complexity of the problem is matched by the array of sophisticated state-of-the-art techniques which have been applied recently (e.g. free-electron laser [21], scanning tunneling microscopy (STM) [22], and storage ring spectroscopy [12]).

2.1 General description of applied methods

To investigate the Jahn-Teller effect appearing in isolated fulleride ions experimentally, the most straightforward method would be spectroscopy in the gas phase. However, according to calculations, only C_{60}^{-} and C_{60}^{2-} ions exist in the gas phase, the other ions emit electrons spontaneously [14]. C_{60}^{-} [12, 21] and C_{60}^{2-} [23, 24] have indeed been prepared in an electron storage ring with long enough lifetime to study their spectroscopic properties.

In solution, all six possible fulleride anions can be prepared and have been studied by various methods. The results are summarized in the review by Reed and Bolskar [18]. The most common reduction methods are the reaction with alkali metals or electrochemistry. In these cases, marked solvent dependence is observed indicating that the effect of the environment is not negligible even in dilute solutions.

In solids, the situation is further complicated by external strain originating from both steric crowding and Coulomb interactions. Roughly two types of fulleride salts can be distinguished: the ones containing bulky organic cations where the ions can be regarded as isolated, but the geometry of the counterions results in a low-

symmetry environment which coexists with the Jahn-Teller type symmetry lowering; and the ones with simple cations (the prime examples being the alkali salts) where the principal interaction is steric crowding when the ions get close).

Since Jahn-Teller distortions involve the deformation of the molecules, structural studies are expected to provide the most straightforward results. These include X-ray and neutron diffraction and tunneling microscopy. Diffraction studies are hindered by the scarcity of suitable single crystals, which would give exact atomic coordinates. On powder samples, Rietveld refinements indicate the deviation from the symmetric shape in one or the other direction, but these results have to be treated with caution because the static or dynamic nature cannot be distinguished. With exceptional care and experimental effort, fulleride monolayers can also be prepared and studied with STM at low temperature where the motion of the fullerene balls is stopped [22].

Inelastic neutron scattering (INS) is suitable to detect librations, low-energy rotational motions in solids. It was used to follow molecular reorientations as a function of temperature [25]. These reorientations should not be confused with pseudorotation as they involve actual displacements of atoms in the crystal; they correspond to an abrupt change in the crystal field [4] and their intensity scales with the crystal field strength.

Vibrational spectra are very sensitive to symmetry changes in a molecule. The splitting of bands in infrared (IR) and Raman spectra correlates with the point group of the molecule which changes when distortions appear. The nature of the splitting, i.e. the number of resulting bands in the distorted state, can be predicted from simple group theory considerations.

Likewise, the electronic transitions between frontier orbitals show characteristic splitting when the symmetry is lowered. These transitions fall into the near infrared (NIR) range in fulleride ions, and are therefore studied by NIR spectroscopy [4, 18].

A special type of measurement is that of ions in the gas phase by intense radiation which causes electron detachment and the absorption spectrum is detected through the deionized molecules it produces. Such radiation sources are either a high-intensity near-infrared laser [12] or infrared radiation from a free-electron laser [21].

High-resolution electron-energy loss spectroscopy (EELS) yields similar information as optical spectroscopy but extends to a much wider frequency range (albeit with lower resolution). Transmission EELS spectra have contributed significantly to our knowledge of fulleride salts [26, 27]. EELS spectra have the advantage with respect to optical spectroscopy that the momentum of the particles and thereby momentum transfer can be controlled; however, since the momentum transfer is always finite, in principle the results cannot be directly compared with those of optical spectroscopy. In practice low-momentum transfer results yield the dielectric loss function with high enough accuracy that it can be subjected to Kramers-Kronig transformation and the complex dielectric function can be derived.

Nuclear magnetic resonance (NMR) spectra can yield information on magnetic properties, rotational states and of the symmetry of both the molecules and their environment. Mostly, ^{13}C is used as a probe, but in alkali salts, alkali atoms as Na or

Li have also been applied. The effect of molecular dynamics, including pseudorotations, on the NMR line shape is thoroughly discussed in Refs. [28, 20].

Electron spin resonance (ESR) is extensively used in the study of fulleride ions, as the magnetic characterization of these molecular ions yields fundamental information on the electronic structure. An ESR signal can in principle appear in any system containing fulleride ions, as the configuration can involve unpaired spins even in systems with an even number of electrons. In solids, the Pauli susceptibility indicates a metallic state.

Indirect but important data on molecular symmetry are provided by transport and magnetic measurements in solids. These properties reflect the collective behavior of electrons in the system, and are indicative of the band structure.

The dynamic nature of the distortion is not always detected by spectroscopy [3]. If the lifetime of the excited state generated during the measurement is shorter than the time it takes the molecule to transform from one distortion to the other, then the molecule can be excited several times while in a single potential minimum. Thus we will measure the spectrum of a distorted molecule. If, on the other hand, the molecule adopts a different distortion faster than the time scale of the measurement, the molecule will take up different distortions during a single excitation event. In this case the spectrum will show the time average of the distortions. As a consequence, it can happen that the molecule is found to be distorted by one measurement and undistorted or even spherical by another; in the solids, where the spatial average is measured as well, different methods can come to different conclusions regarding whether the material consists of identically distorted molecules (cooperative Jahn-Teller effect) or whether the spatial average is symmetric while the individual molecules perform random motions (dynamical Jahn-Teller effect) [16].

Despite the difficulties mentioned above, by now a critical mass of data has been compiled enabling us to formulate a concise picture of the nature of the JT effect in these fascinating materials. In the rest of this paper we would like to summarize such experimental data with respect to the following questions: Are the fulleride ions found in various compounds distorted? Is the distortion dominated by the molecular Jahn-Teller effect or by the potential field of the environment? In which direction is the molecule distorted and what is the shape of the distortion? Is the distortion static or dynamic? The way we approach these questions is the study of symmetry change through vibrational and electronic transitions. The fundamental concepts of these methods will be summarized in the next section.

2.2 Vibrational and electronic spectra of fulleride solids

C_{60} has four infrared allowed vibrations, all of which belong to the T_{1u} representation. The correlation table (Table 1) lists the possible splitting in various point groups describing the molecule when the icosahedral symmetry is lost. Since the LUMO of the molecule which accomodates the extra electrons in the anions, is also a t_{1u} orbital, the same correlations hold for the electrons as well. The result-

ing schemes are shown in Fig. 3 for different occupation numbers 0-6 [29]. These schemes are based on the calculations of Auerbach et al. [7] for isolated anions with correlations between electrons neglected. This calculation resulted in low-spin states for all ions which, because of the full occupation of the lowest levels, are not subject to further JT activity.

Table 1 Correlation table for the T_{1u} representation. The correlation table for the T_{1g} representation is identical, with the indexes u changed to g.

I_h	D_{5d}	D_{3d}	D_{2h}
T_{1u}	$A_{2u} + E_{1u}$	$A_{2u} + E_u$	$B_{1u} + B_{2u} + B_{3u}$

It is apparent from table 1 that while D_{3d} and D_{5d} symmetries retain a double degeneracy, in D_{2h} all representations are one-dimensional, thus the entire degeneracy is lifted. In practical terms, this means that in an infrared spectrum the four allowed modes would show two- or threefold splitting depending on the symmetry resulting from the distortion. Because of the usually small structural changes, the split infrared bands are expected in the immediate vicinity of the original T_{1u} frequencies. Upon symmetry lowering, silent modes also become activated, but for the purpose of identification the splitting pattern of the T_{1u} modes is the least ambigous. Among these, the highest-frequency $T_{1u}(4)$ mode is the most characteristic; this mode is not only sensitive to symmetry through splitting, but also to the charge of the anion through its downshift in frequency from the 1429 cm^{-1} position in neutral C_{60} [30].

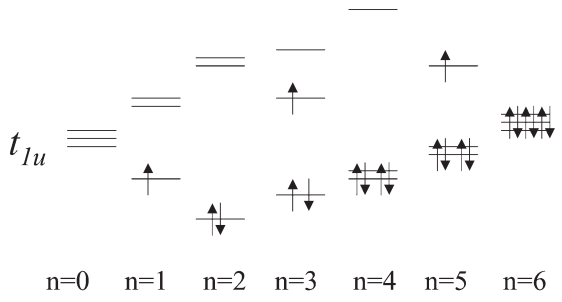

Fig. 3 Jahn-Teller splitting of the t_{1u} orbitals of C_{60}^{n-} [29]. Copyright (2002) by the American Physical Society.

Further symmetry reduction can happen as a result of strain from the crystal field of the cations in crystals. If the site symmetry of the fulleride ion is a subgroup of the

I_h icosahedral point group, with lower symmetry than the JT distorted shape (e.g. C_{2h}), a simple symmetry lowering occurs to the shape dictated by the site symmetry. If the site symmetry is not a subgroup, the distortion happens into the highest common subgroup of the site symmetry and the icosahedral group. Examples of such distortions will be given when discussing the specific materials.

It is worth mentioning that although the I_h point group shows a very high symmetry, it lacks a fourfold axis. The structure of many fulleride salts, though, which contain the ions in a tetragonal cation environment, can be described as tetragonal based on diffraction data. This can only happen when the fullerene cages are disordered with respect to the C_2 axis which is parallel to the principal axis of the crystal. Formally, the picture is often described as the sum of two perpendicular orientations (the so-called "standard orientations"), but from structural data it cannot be decided what exactly the shapes are, or even whether the disorder is static or dynamic. We will show examples of mono- and tetravalent salts where this orientational disorder occurs. It is expected that in such cases vibrational spectroscopy yields more precise information on the shape of the molecular ion and thus the type of the disorder.

The splitting of the electronic orbitals (Fig. 3) also gives rise to additional structure in the electronic spectra. The transitions between levels in the figure are dipole-forbidden and thus cannot be detected by optical methods; however, excitations to the LUMO+1 t_{1g} level, which will also split in a lower symmetry environment, will show characteristic structure depending on the shape of the fullerene cage. We will give an example of such analysis in section 3.2.1.

3 Results on fulleride salts

In this section we present the results on fulleride salts in various charge states. The grouping is not strictly in the order of increasing charge, for both fundamental and practical reasons. The main practical reason is the scarce availability of some groups of the fulleride family. Of the alkali salts, A_2C_{60} (except for Na_2C_{60}) and A_5C_{60} were found to phase separate, and could not be prepared even in a segregated form. Na_2C_{60} is a nanosegregated mixture at room temperature and the JT features can only be studied in its high-temperature phase [31].

We will not cover the optical properties of superconducting A_3C_{60} salts, either, both because the theoretical implications of the Jahn-Teller effect on superconductivity has been extensively discussed [32] and because experimental spectra in these compounds concentrate on electronic effects [33] and vibrational spectra have not been discussed in detail, partly because of the interference with the background of free electrons.

We will concentrate on the monovalent and tetravalent systems where enough data exist to present a consistent picture based on optical spectra but in accordance with other experimental results.

3.1 C_{60}^-

In the C_{60}^- anion in the gas phase the presence of the dynamic Jahn-Teller effect has been shown by sophisticated measurements in both the NIR [12] and the MIR [21] spectral range. In both cases, it was found that the pseudorotation of the molecules is fast enough to yield the spectrum of an undistorted ion. The multiple pattern found in the NIR spectra[12] was attributed to transitions between pseudorotational levels.

In solutions or in frozen matrices the effect of the environment is not negligible any more. The NIR spectra of C_{60}^- were measured in various frozen noble gas matrices [34] and D_{3d} or D_{5d} distortions were found. The result was the same in the apolar methylcyclohexane matrix, while the distortion was D_{2h} in the polar 2-methyltetrahydrofuran (2-MeTHF) matrix [35]. One might expect the same polarity dependence in solutions, but electrochemically generated C_{60}^- ions showed a NIR spectrum consistent with D_{5d} and D_{3d} symmetry both in benzonitrile and in dichloromethane [36]. These findings indicate that the symmetry of the environment has to be taken into account besides simple polarity considerations in frozen matrices [37] and in solutions.

A static-to-dynamic transition was also observed in Na(dibenzo-18-crown-6)C_{60} in frozen 2-MeTHF solution [37]. The ESR spectrum showed an ellipsoidal distortion of the C_{60}^- ion at low temperature, and heating lead to an isotropic signal.

Another possibility to measure nearly isolated fulleride ions is the investigation of solid fulleride salts with bulky cations. The large cations separate the fulleride ions but in many cases they are capable of lowering their symmetry at the same time. In $Ni(C_5Me_5)_2C_{60}$ the C_{60}^- ion was found by X-ray diffraction to be oblate shaped and to have roughly D_{2h} symmetry [38]. This results probably from the enhanced $\pi - \pi$ interaction between the C_5Me_5 and the fullerene units.

In (TDAE)C_{60} (TDAE=tetrakis-dimethylaminoethylene) the Jahn-Teller effect has an intriguing consequence [20]: it results in a ferromagnetic ground state with a Curie temperature T_c = 16 K [39]. The temperature dependence of the correlation time of pseudorotation from 5-20 K was obtained from ^{13}C NMR measurements [28] and was found to decrease from 10^{-6} s to 10^{-7} s.

Salts formed with the metalloorganic cations tetraphenylphosphonium and tetraphenylarsonium can be prepared as relatively large crystals by electrochemical methods and are not air sensitive, contrary to the other monoanionic fullerides mentioned above; as a consequence, they have been extensively studied by several methods [41, 42, 43, 40, 44]. The composition of the crystals is always two counterions to one fulleride monoanion, and charge neutrality is preserved by one halide ion (Cl^-, Br^- or I^-) per fulleride ion. The type of the halide ion depends on preparation conditions and can be homogeneous or a mixture of two kinds of halides. This fact introduces an additional disorder into the structure, but as we will see, its impact is relatively weak.

The most thorough structural study has been performed by Launois *et al.*[40] by single-crystal X-ray diffuse scattering and diffraction. Above 130 K, the structure was identified as tetragonal ($I4/m$), arising from a superposition of two orientations

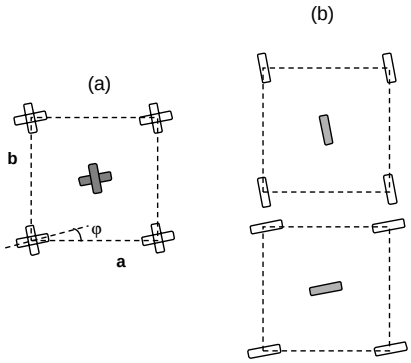

Fig. 4 Schematic models of $(Ph_4)_2PBrC_{60}$ at a) high temperature and b) low temperature. Reprinted from [40]. With kind permission of The European Physical Journal (EPJ).

of the fullerene anion. (As the icosahedral C_{60} molecule has no fourfold axis, this is the way to explain its presence in a tetragonal environment.) Below 120 K, the model which could explain diffuse scattering was that of separate domains of $I2/m$ symmetry, which is consistent with a C_{2h} distortion of the fulleride anion. This is another example of Jahn-Teller distortion complemented by external strain: interaction of the electrons with vibrations of h symmetry should result in no lower than the D_{2h} point group [3], but since the C_{60}^- ions occupy sites of $2/m$ (C_{2h}) symmetry, their point group has to be lowered accordingly.

The situation is illustrated in Fig. 4. In part a), the structure is the dynamic average of two standard orientations, differing in the direction of one of the fullerene axes (it is easiest to associate this direction with that of the bond separating two hexagons, intersected by a C_2 axis, depicted on the right of Fig. 1). In part b) the structure is envisaged to consist of independent domains, including fulleride ions of C_{2h} symmetry but of different orientations. Within the domains, the cooperative Jahn-Teller effect is realized; however, the whole crystal is not uniform but disordered.

Bietsch *et al.* [43] determined the g-factor anisotropy of $(Ph_4P)_2P(As)C_{60}(I,Cl)$ as a function of temperature. Their results complement perfectly the structural data: the g-factor is isotropic above a specific temperature (As: 125 K, P: 142 K) where it becomes anisotropic and the principal axes of the g-tensor do not coincide with the crystal axes.

Infrared spectra also show line splittings indicating a deformation in both tetraphenylphosphonium [42] and tetraphenylarsonium [44] salts. The main conclusion of the first paper is that in contrast to ESR spectra, infrared lines still show a splitting due to deformation at room temperature, indicating a dynamic JT state; nevertheless, some of the lines, including counterion modes, exhibit anomalies in their temperature dependence around the ordering transition temperature (Fig. 5). A thorough combined experimental and theoretical study has been performed in the second pa-

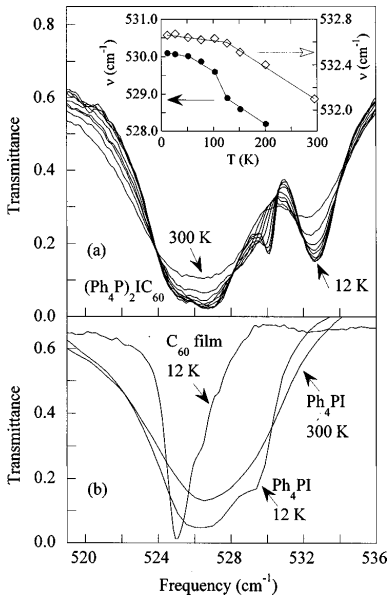

Fig. 5 Temperature dependence of a) the $(Ph_4P)_2IC_{60}$ multiplet and b) the pristine C_{60} and Ph_4PI absorbances which contribute to it. The inset in a) shows frequency versus temperature for the high ν side of the $T_{1u}(1)$-derived doublet (open diamonds) and the 530 cm^{-1} counterion feature (solid circles), with solid lines to guide the eye. Reprinted from [42]. Copyright (1998) by the American Physical Society.

per, concluding that the most probable deformation of the C_{60}^- anion is either C_{2h} with the principal axis connecting the centers of two opposite pentagons ($C_{2h,5}$) (according to the D_{5d} symmetry undergoing further distortion to C_{2h}) or C_i. C_{2h} symmetry is compatible with both the site symmetry $2/m$ and the result from the g-factor anisotropy [43], but the calculated vibrational fine structure assuming C_i symmetry agrees more with the experiment. A further reduction in symmetry can of course easily happen in such a complicated crystal and since both point groups contain one-dimensional representations, more subtle effects have to be taken into account in both theory and experiment.

Likewise, room-temperature Raman spectra of single crystals of tetraphenylphosphonium salts with all three halide ions [45] showed a broadening of H_g lines which can be fitted with five oscillators. This indicates the lifting of the fivefold degeneracy, which is the case in C_{2h} (or lower) symmetry.

The exact temperature of the phase transition in the experiments above is subject to some uncertainty, which we attribute to the stoichiometric variations in both the central atom of the counterion (P,As) and the type of the halide. The picture that emerges, however, is compatible with the full scope of experimental results: a dynamic Jahn-Teller effect at high temperature, a structural phase transition in the 120

- 150 K range, and a distortion of the molecular ion in the low-temperature phase, arising from the positive synergy of the cooperative Jahn-Teller effect and the low symmetry of the environment. The static-to-dynamic transition does not coincide with the structural transition and its temperature depends on the detection method: whereas ESR spectra are isotropic at room temperature, infrared lines are still split, indicating a distorted state on the time scale of the measurement. This phenomenon puts the time scale of the pseudorotation between 10^{-9} and 10^{-13} s, respectively.

We can compare the above results to those of TDAE-C_{60} investigated by nuclear magnetic resonance [28, 20]. In these studies, based on NMR line shape analysis, a static-to-dynamic transition has been found in the ferromagnetic phase, below 10 K. The time scale at this temperature of the pseudorotation was estimated as 3 ns, somewhat higher than the higher limit of the room-temperature range mentioned above. Even though the systems are not identical, the qualitative picture that emerges is in accordance with the transition occurring in the order of characteristic frequencies (NMR $\rightarrow$ ESR $\rightarrow$ IR). An attractive model has been proposed for the magnetic ordering of fulleride monoanions in this salt, based on Jahn-Teller distorted states [20]: according to the calculations of Kawamoto [46], ferromagnetic order develops if the principal axes of neighboring C_{60}^{-} ions are perpendicular, whereas antiferromagnetic order results from parallel ordering of the principal axes. A cooperative but complex Jahn-Teller state consisting of molecular ions ordered perpendicularly thus could show ferromagnetism which would disappear at the temperature where the system becomes dynamic due to increased pseudorotation frequency.

Unfortunately, the simplest fulleride salts, the monovalent AC_{60} (A=K,Rb,Cs) alkali fullerides, exist in a polymerized phase at room temperature (see section 4.2) and depolymerize only above 400 K where the rotation of the balls averages out any distortion. Infrared spectra of monoanions at this high temperature show unperturbed icosahedral symmetry [47, 48].

3.2 C_{60}^{4-} and C_{60}^{2-}

We begin this section with the discussion of C_{60}^{4-} systems, because these are the ones where experimental results are abundant. Among the non-superconducting systems, the tetravalent salts were studied most thoroughly both experimentally and theoretically. Several factors contributed to this fortunate situation. On the materials side, the full series of A_4C_{60} (A = Na, K, Rb, Cs) could be prepared as single-phase powders, and except for Na_4C_{60} which is a polymer at room temperature, proved to be similar in structure and properties. On the theory side, the controversy between band structure calculations predicting metallic behavior [49] and the insulating character found experimentally has been noticed early on and has led to extensive effort to resolve it.

C_{60}^{2-} was thought to be the electron-hole analogue to C_{60}^{4-} and studies on these materials could have complemented the C_{60}^{4-} results with valuable information. Unfortunately, only Na_2C_{60} could be prepared so far and that material is not single

phase at all temperatures, either. We will report our results regarding the JT effect and the other intriguing properties of this system after discussing the tetravalent alkali salts, which are the most complete series for conclusions about the JT effect to be drawn.

3.2.1 C_{60}^{4-}

Both in solutions [36] and in a solid with large organic cations [50] the C_{60}^{4-} ions were shown to be distorted. A low temperature STM study on K_4C_{60} monolayers also showed distorted fulleride ions. The ground state of both $[Na(crypt])_4C_{60}$ [50], K_4C_{60} [51] and Rb_4C_{60} [52] was shown to be singlet (Fig. 3.), with a close-lying triplet excitation, in accordance with the distortion.

The molecular Jahn-Teller effect plays an important role in determining the electrical and magnetic properties of solid A_4C_{60} and A_2C_{60} salts. This is because electron correlation localizes the electrons on the fulleride ions; these solids can be described as nonmagnetic Mott-Jahn-Teller insulators [16]. Intersite electron repulsion (U) localizes the electrons and leads to the observed insulating behavior [53, 54, 55], while the Jahn-Teller splitting leads to a nonmagnetic ground state [51] pairing the electrons in contempt of Hund's rule.

In contrast to the A_4C_{60} salts, monomeric Na_4C_{60} – stable above about 500 K – is a metal. The reason is that the shorter interfullerene distances of this compound reduce the Hubbard U and increase the bandwidth W, leading to an U/W value lying in the metallic domain [56]. Li_4C_{60} also has a metallic monomer phase above 470 K [57, 58]. The presence of distorted fulleride ions has not been investigated in these phases yet.

K^+, Rb^+ and Cs^+ form salts with C_{60}^{4-} which contain monomeric fulleride ions at all temperatures. The structure of these salts is $I4/mmm$ body centered tetragonal (bct) structure at all temperatures [4, 59, 60], except Cs_4C_{60} at room temperature and below, which is *Immm* orthorhombic (bco) [61]. According to our present knowledge, the fulleride ions in these phases are not rotating [4, 60]. Thus the effect of the crystal field must be taken into account.

In the bct phase the nearest cations surrounding a C_{60}^{4-} ion form a D_{4h} structure (see Fig. 6). As the fulleride ion does not have a fourfold rotation axis, it cannot distort into this point group (see section 2.2). In this case the molecule has to distort into the largest common subgroup of D_{4h} and I_h, which is D_{2h}. The three twofold rotation axes of the D_{2h} distorted molecule can then coincide with those of the crystal. The overall tetragonal structure is realized in a way similar to $(Ph_4P)_2C_{60}$, with two standard orientations (Fig. 4a), but in this case the angle ϕ is zero.

In the bco phase of Cs_4C_{60} the cations show a similar arrangement as in the bct A_4C_{60} phases, but they form a D_{2h} structure, i.e. they allow only one orientation of the fulleride ions. Thus the *molecular* point group caused by the crystal field is D_{2h} in both the bct and the bco structure and we would expect identical molecular spectra.

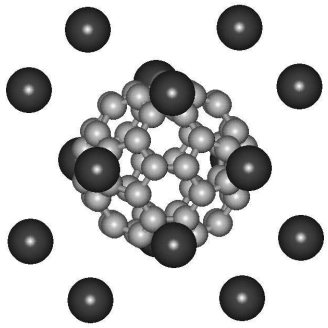

Fig. 6 A C_{60}^{4-} ion (in light grey) and its nearest neighbor K^+ ions (in black) in the bct A_4C_{60} salts (based on [59]). The fourfold *c* axis of the crystal is perpendicular to the plane of the paper, whereas the *a* axis is horizontal and the *b* axis vertical. The size of the spheres denoting the atoms is not to scale.

As we have seen in Sect. 1. the molecular Jahn-Teller effect distorts the molecule into either D_{3d} or D_{5d} symmetry. It is not impossible to place such distorted anions in a lattice so that the overall symmetry remains tetragonal, but the main axis of these distortions cannot coincide with the principal crystallographic axis of the A_4C_{60} crystals. In line with the suggestions by Fabrizio and Tosatti [16], the main distortion axis of the molecule could be disordered or ordered in some way, but the average structure has to be that found by diffraction.

The competition between the strain caused by the crystal and the molecular degrees of freedom producing the JT distortion results in several phases in A_4C_{60} salts. In the following sections we will discuss these different phases and their phase transitions.

Orthorhombic A_4C_{60} phases

No single crystals were grown from these materials, and only powder diffraction experiments could be performed. From these measurements the distortion of the C_{60}^{4-} ion could only be determined in bco Cs_4C_{60} [60]. The point group of the fulleride ion was found to be D_{2h} in accordance with the symmetry of the crystal field. Nevertheless, the C atoms which were the most further apart from the icosahedral geometry were not found in the direction of the longest crystallographic axis. Thus the distortion is dominated by the crystal field, but the role of the Jahn-Teller effect is also significant [60].

The MIR spectrum of Cs_4C_{60} contains a threefold split $T_{1u}(4)$ peak below 400 K (Fig. 7.c.) [4]. This also corresponds to a D_{2h} distortion (see Table 1.). Magic angle spinning (MAS) NMR experiments could also detect the distorted geometry of the C_{60}^{4-} ion in Cs_4C_{60} at room temperature [62]. In the NIR spectrum of the fulleride ions we find peaks corresponding to transitions between the split $t_{1g} \leftarrow t_{1u}$

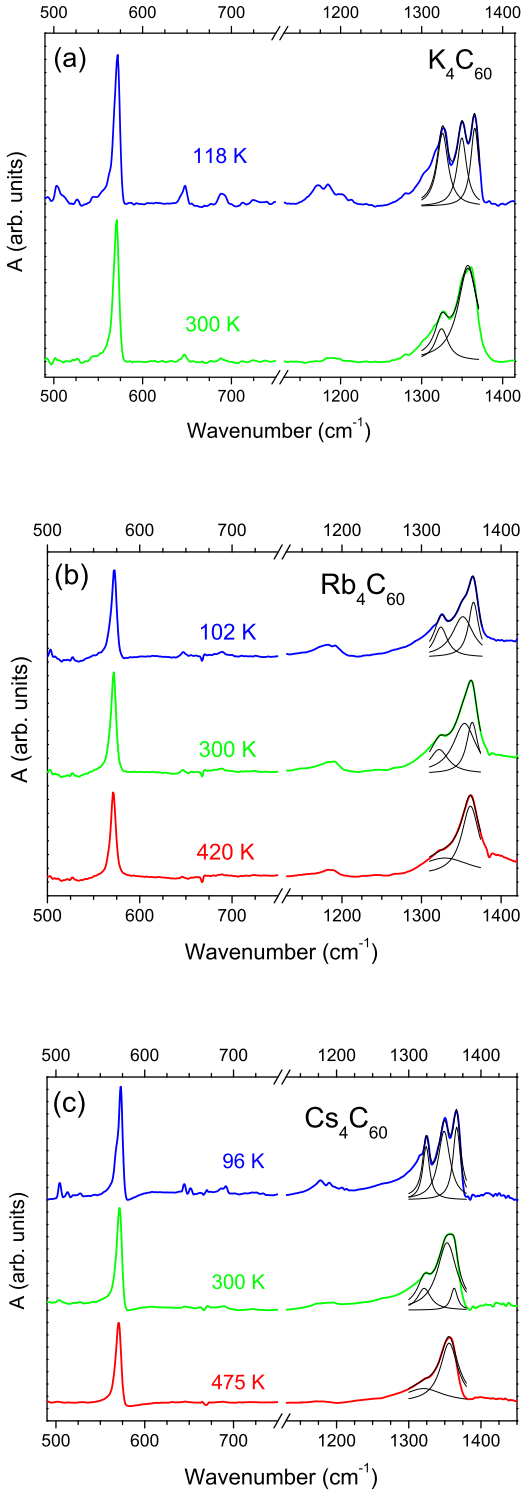

Fig. 7 MIR spectrum of (a) K_4C_{60}, (b) Rb_4C_{60}, and (c) Cs_4C_{60} at selected temperatures. The $T_{1u}(4)$ mode can be fitted with three Lorentzians at low temperature and two Lorentzians at high temperature (black lines). These splittings indicate a molecular symmetry change with temperature. [4] Copyright (2006) by the American Physical Society.

orbitals [27]. The number of detected transitions correlates with the point group of the molecule (see Fig. 8). As the NIR spectrum of the bco phase of Cs_4C_{60} contains four peaks (Fig. 9.b.), the point group of the C_{60}^{4-} ion cannot be higher than D_{2h} [4], in agreement with the above explained measurements.

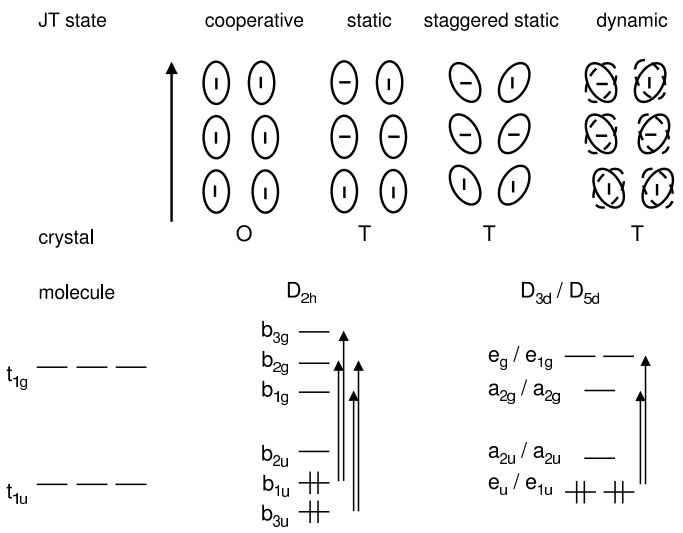

Fig. 8 Upper panel: schematic representation of fulleride ion orientation in various Jahn-Teller states. The arrow indicates the crystallographic *c*-axis, the bars in the ovals the orientation of a hexagon-hexagon double bond. Lower panel: The split frontier MOs of the C_{60}^{4-} ions and the dipole allowed transitions indicated by arrows. For comparison we depicted these MOs for the I_h C_{60}, as well. The ordering of the b_{1-3u} and of the b_{1-3g} orbitals is arbitrary. [4] Copyright (2006) by the American Physical Society.

Under pressure Rb_4C_{60} undergoes a phase transition to an orthorhombic phase similar to that of Cs_4C_{60} [63]. Previously it was believed that Rb_4C_{60} transforms into a metallic phase under pressure [64]. In a recent thorough study, though, no such transition has been found up to 2 GPa [65]. The nature of the fulleride ion distortion in the orthorhombic Rb_4C_{60} is as yet unknown.

K_4C_{60} and Rb_4C_{60} at low temperature

In the static ^{13}C NMR spectrum of K_4C_{60} and Rb_4C_{60} a continuous broadening from about 15 ppm to about 200 ppm was found on cooling [51, 64]. According to

Kerkoud et. al. the low temperature broad peak arises from the superposition of the 9 inequivalent C atoms of a D_{2h} distorted molecule [64].

The D_{2h} distortion of the fulleride ions was also confirmed by MIR and NIR spectroscopy in K_4C_{60} below about 270 K and in Rb_4C_{60} below about 330 K [4]. Both the MIR and NIR spectra show similar splittings as in Cs_4C_{60}, although the crystal structure is different (see Figs. 7. and 9.) [4]. As we have seen above, this symmetry can be regarded as proof for crystal-field dominated distortion.

A_4C_{60} at high temperature

In K_4C_{60} at room temperature the positions of the C atoms could not be derived from diffraction measurements, but it was shown that the distortion is quite small: the difference between the axial and the equatorial axis of the molecule is smaller than 0.04 Å [66].

The detection of a dynamic distortion is complicated by the fact that measurements with a short characteristic time scale will detect the molecule to be symmetric, therefore they will not prove the presence of the distortion. This can be the situation of NMR at room temperature. Both in K_4C_{60} and in Rb_4C_{60} all C atoms of the C_{60}^{4-} molecule were found to be identical by ^{13}C MAS NMR, i.e. the molecule was detected to be icosahedral [67]. Above 350 K MAS NMR also detected a single C line in Cs_4C_{60}, although this was explained by the starting of the rotation of the fulleride ion [62].

The Raman spectrum of the A_4C_{60} materials did not show a splitting, which would have shown the symmetry lowering of the fulleride ion [61, 68], although the lines were found to broaden.

The timescale of infrared spectroscopy is such that it is capable of detecting dynamic distortions. This method is sensitive to the local structure, so that it detects the distortions of the single molecules and not their average. The MIR spectra of the A_4C_{60} compounds at high temperatures show a twofold split $T_{1u}(4)$ mode (Fig. 7) corresponding to either a D_{3d} or a D_{5d} distortion (see Table 1.) [4, 69]. The NIR spectra contain two peaks (Fig. 7), which also correspond to D_{3d} or D_{5d} structures (see Fig. 8.) [4]. These are the distortions favored by the molecular Jahn-Teller effect. It has been shown that at high temperatures these distortions are dynamic [4].

Static-to-dynamic transition

We propose the following explanation for the transition between the static and dynamic state [4, 70]: At low temperature the distorting potential field of the cations is strong, leading to an APES where the lowest minimum has D_{2h} symmetry. As at low temperature only the lowest energy states are occupied, no transition can take place to other higher lying minima. On heating two processes have to be taken into account. The first is caused by the thermal expansion: the steric crowding decreases and the potential energy minimum created by the crystal field will become more

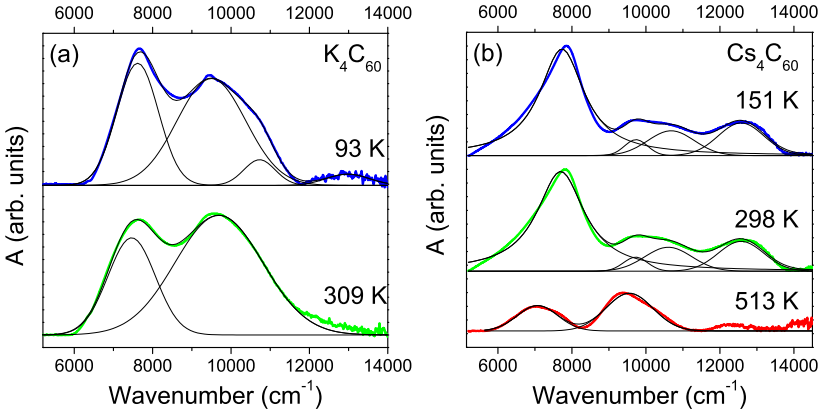

Fig. 9 Baseline-corrected NIR spectrum of (a) K_4C_{60}, and (b) Cs_4C_{60} at selected temperatures. The spectra were fitted with Gaussians, with the exception of the lowest frequency peak of Cs_4C_{60} at 151 K and 298 K where a Lorentzian produced a better fit. These fits are shown with black lines. [4] Copyright (2006) by the American Physical Society.

shallow. The other effect is that more higher lying states will become thermally accessible. These two factors lead to the gradual appearing of D_{3d}/D_{5d} distortions and disappearing of the D_{2h} distortions, until only the former will be present. Of course if there is a phase transition, like in Cs_4C_{60} on heating, that overrides the gradual nature of this scenario.

D_{3d}/D_{5d} distortions in different directions have different energy in the solid, due to an additional anisotropic term from the crystal field. The appearance of the D_{3d}/D_{5d} distortions starts with the lower energy ones, connected by possible pseudorotation. On heating the confinement of the pseudorotation relaxes as more and more D_{3d}/D_{5d} distortions become accessible, until at high temperatures the pseudorotation will become free.

The main process which emerges is that the fulleride ion can be thought of as an independent entity, which undergoes a distortion even in the absence of external strain. If we put this ion into a crystal with a given symmetry, a competition between the molecular degrees of freedom and the constraints of the environment will result. The molecular degrees of freedom will gain in importance when the kinetic energy is higher (at higher temperature) or when the constraint is lower (the lattice is less crowded). The increase of the transition temperature with cation size is in agreement with this picture.

3.2.2 C_{60}^{2-}

The geometry of the C_{60}^{2-} ion in its benzonitrile and dichloromethane solution was found by NIR spectroscopy to be D_{3d} or D_{5d} [36]. A D_{3d} distortion was also found

in $(ND_3)_8Na_2C_{60}$ by diffraction measurements [71]. This latter distortion must be static, since diffraction can only detect such distortions.

In contrast to these findings probably the symmetry lowering effect of the counterions is reflected in the C_i distortion found in $(PPN)_2C_{60}$ (PPN^+ = bis-(triphenylphosphine)iminium ion) by X-ray diffraction. The shape of the deformation is an axial elongation with a rhombic squash [72].

To study the Jahn-Teller effect of fulleride ions in the condensed phase a symmetric environment would be ideal. Na_2C_{60} was reported to be cubic: simple cubic below 319 K and face centered cubic (fcc) above [73, 74]. In the fcc phase the C_{60}^{2-} ions are rapidly rotating [73, 74], thus the crystal field acting on the fulleride ion is spherical. Unfortunately, though, Na_2C_{60} shows nanosegregation below 460 K and the phase containing C_{60}^{2-} ions appears only at high temperature [31].

The Jahn-Teller effect overrides Hund's rule and the ground state of the C_{60}^{2-} molecules is a singlet with a low lying excited triplet state [18, 51] (Fig. 3.). Thus Na_2C_{60} is nonmagnetic [51].

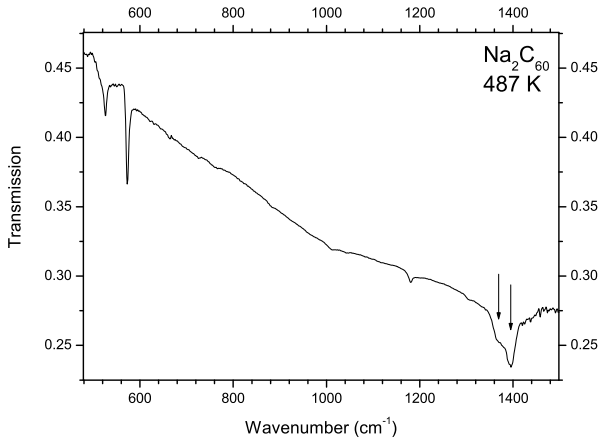

Fig. 10 MIR spectrum of Na_2C_{60} at 487 K. The twofold splitting of the $T_{1u}(4)$ mode due to the Jahn-Teller effect is shown by arrows. Reprinted from [70]. Copyright (2007) Elsevier Science.

We have studied the Jahn-Teller effect in this phase by MIR spectroscopy [31, 70]. The $T_{1u}(4)$ mode shows a twofold splitting and modes that are silent in C_{60} appear, indicating a D_{3d} or D_{5d} distortion of the molecule (Fig. 10). As the C_{60}^{2-} ions are rotating in this phase [73, 74], the distortion cannot be caused by the crystal field but must be due to the molecular Jahn-Teller effect. As there is no crystal field to lock the C_{60}^{2-} into a single potential well, the distortion is dynamic, with the rate of pseudorotation smaller than that of the infrared measurement.

This latter result proves beyond doubt that fulleride anions can be regarded as preserving their molecular identity. To show lower symmetry without a constraining crystal field cannot be explained by any other mechanism.

From the data on divalent and tetravalent salts, a consistent picture emerges which is in perfect agreement with the Mott-Jahn-Teller insulator model of Fabrizio and Tosatti [16]. The Jahn-Teller distortion, even if dynamic, can be unambigously detected from vibrational and low-energy electronic spectra and proves that the molecular JT effect causes the nonmagnetic insulating behavior in these materials. Systems with smaller cations are on the metallic side of the U/W diagram; it would be of interest to study these systems by vibrational spectroscopy as well.

3.3 C_{60}^{3-}

In the work of Lawson et. al. a NIR spectroscopic evidence was found for the distortion of C_{60}^{3-} ions in benzonitrile and in dichloromethane solution [36]. The point group of the molecule is not known, but it is such that its irreducible representations are all nondegenerate. The ground state of the C_{60}^{3-} molecule is S=1/2 [18] also indicating the splitting of the t_{1u} orbitals (Fig. 3.) This low-spin state was found in $Li_3(NH_3)_6C_{60}$ [75] as well, despite the fact that the fulleride ions are surrounded by a bcc lattice, where no crystal field splitting of the t_{1u} orbitals is expected. This shows the Jahn-Teller origin of the splitting in C_{60}^{3-}.

In contrast to the above results, no Jahn-Teller distortion was found in metallic A_3C_{60} compounds. The geometry of the fulleride ion was measured in K_3C_{60} by neutron powder diffraction at room temperature, and it was found to belong to the T_h point group [76]. The low-temperature STM study on monolayers of K_3C_{60} by Wachowiak et al. [22] found undistorted molecules in the topographic image and a metallic band structure by tunneling spectroscopy. No splitting was found in the MIR and NIR spectra of these compounds, either [30, 69]. Careful comparison of several C_{60}^{3-}-containing salts by Iwasa and Takenobu [77] led to the conclusion that high-spin orbital degeneracy can prevail in these systems, provided the anions are sufficiently close and the environment is symmetric enough. The degeneracy breaks down when ammonia molecules are inserted into the structure and either increase the distance or lower the symmetry; in this case, the metallic behavior is also lost and the system becomes an insulator without a superconducting transition.

To understand the coexistence of metallicity and symmetry, we can look at the Mott-Jahn-Teller picture starting from a collective electron system, instead of building up the solid from individual JT distorted molecular ions. (Such a reasoning is given very clearly by Dahlke et al. [60].) If we imagine a metallic solid where the atomic cores are replaced by C_{60} molecules and all extra electrons are delocalized, the closed-shell cores will not be subject to distortion. As soon as localization occurs, the t_{1u} LUMO's will be occupied and the usual JT effect takes place. The borderline between the two scenarios is the critical U/W value between the metallic

and Mott-Hubbard insulating state. It seems that in fullerides this critical value depends on both the charge of the anion and the cation-anion distance and A_3C_{60} salts with A = K and Rb are already on the metallic side, whereas even-charged systems are on the insulating side; however, the boundary seems to be very close as the example of Na_4C_{60} and Li_4C_{60} shows. Further details could be provided by combined spectroscopic and theoretical efforts.

Since there is near consensus about the mechanism of superconductivity in these compounds being related to electron-phonon coupling, there were many attempts to relate this mechanism to the Jahn-Teller effect. The topic is summarized extensively in the work of Gunnarson [32]. Han, Gunnarson and Crespi [78] presented a particularly appealing model of the connecting superconducting pairing with the Jahn-Teller effect. In their picture, the electron pairs formed by the JT effect in C_{60}^{3-} are mobile and constitute the pairing mechanism required by superconductivity. Since the JT stabilization energy for anions with even-numbered electrons is much larger, the pairs there will be localized and superconductivity will not occur. A further advantage of the model is that it is also in accordance with other special properties of fulleride superconductors as e.g. the short coherence length.

4 Unusual phases: why do we not see isolated fulleride ions in alkali salts?

We have seen above that close-lying thermally accessible orbitals can give rise to many unusual phenomena in fulleride solids. We now briefly discuss two further consequences of the presence of such states: possible chemical reactions (as e.g. polymerization) and the coexistence of several phases in a solid at the same temperature (segregation). Both are a source of new information but unfortunately they also prohibit a full systematic investigation of the monomeric alkali fulleride salts series.

4.1 Segregation

The first example of segregation in fullerides was the so called intermediate phase of KC_{60} [79]. In this material the K^+ ions are not homogeneously distributed in the C_{60} lattice : there are regions of pure neutral C_{60} and regions with a composition of K_3C_{60}. Synchrotron X-ray diffraction measurements showed the different lattice constant of the regions with different compositions [79]. It was found that the lattice of the C_{60} region, which has smaller lattice parameter, expands (a = 14.18 Å instead of 14.14 Å) and the lattice of K_3C_{60} contracts (a = 14.22 Å instead of 14.25 Å). The MIR spectrum shows vibrational lines characteristic of C_{60} and of C_{60}^{3-} (Fig. 11.) On heating the material above 460 K, the segregation disappears and a KC_{60} phase with C_{60}^{-} ions appears [79].

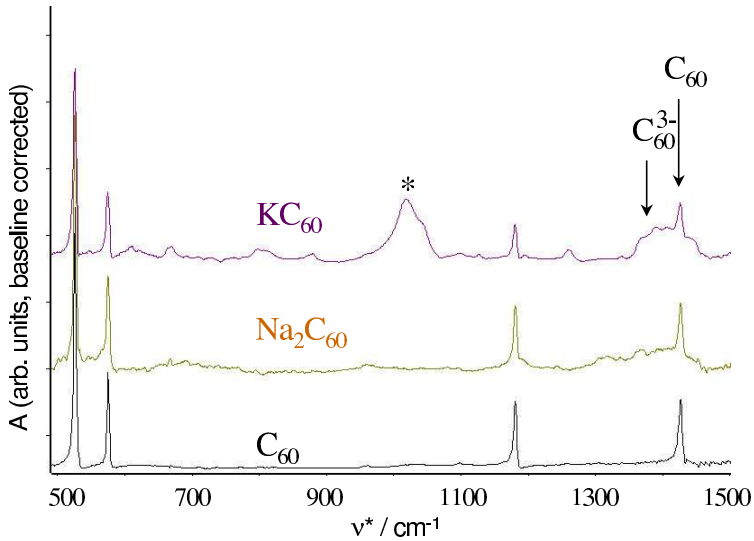

Fig. 11 Baseline-corrected MIR spectrum of KC_{60} and Na_2C_{60} compared to the spectrum of C_{60}. The line positions characteristic of neutral C_{60} and of C_{60}^{3-} molecules are shown. Amorphous carbon impurity in the KC_{60} sample is denoted by an asterisk.

A similar segregated structure is present in Na_2C_{60} at room temperature [31]. This structure consists of C_{60} and the Na_3C_{60} regions with the size of about 3-10 nm. X-ray diffraction could not distinguish the two lattice constants in this case, probably because of the closeness of the two lattice parameter values of the parent lattices ($a(C_{60})$ = 14.15 Å and $a(Na_3C_{60})$ = 14.19 Å). The presence of C_{60} and Na_3C_{60} was proven by a combined effort using ^{13}C NMR, ESR and MIR spectroscopy and neutron scattering (Fig. 11.) On heating the Na^+ ions start to diffuse and the composition of the whole material becomes homogeneous. This is the phase where Jahn-Teller distorted C_{60}^{2-} ions were found [31].

Segregation was also proposed in Na_3C_{60} based on the presence of C_{60} seen by ^{13}C NMR. This material was also detected to be single phase by x-ray diffraction [80].

4.2 Polymerization

For the fulleride ions to polymerize two conditions have to be met: the molecules have to be close enough to each other, and they have to be in adequate orientation. The type of bonding depends on the charge of the fulleride ion [81]. Neutral C_{60}

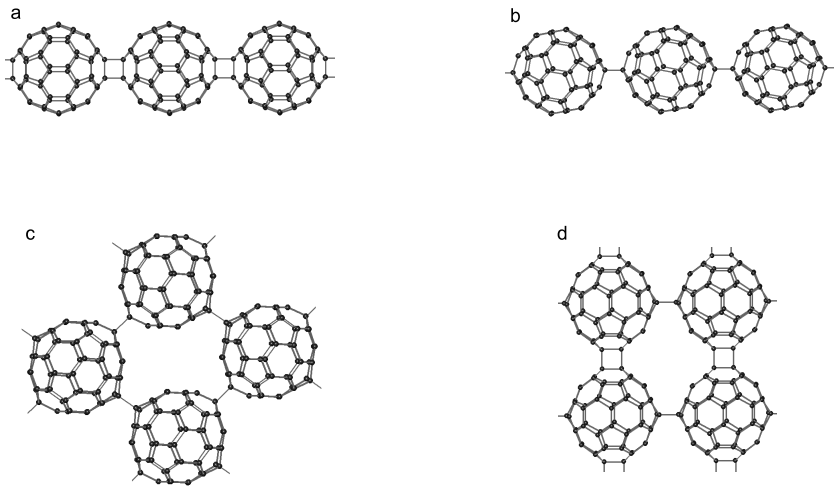

Fig. 12 Bonding of fulleride ions in various polymers. a: AC_{60}, b: Na_2AC_{60}, c: Na_4C_{60}, d: Li_4C_{60}.

and C_{60}^{-} favor chains with [2+2] cycloadditional bonds. The former can be found in the C_{60} photopolymer [82], and the latter in AC_{60} polymers [83]. AC_{60} (Fig. 12a.) were the first ionic polymers discovered and were extensively studied due to their stability in air. They undergo reversible depolymerization between 450 and 480 K and can be quenched into a metastable dimer phase [84] with bonds similar to those in Fig. 12b [85].

The most stable bonding pattern of $(C_{60}^{3-})_n$ is a linear chain with single interfullerene bonds (Fig. 12b.) [81], which can be found in Na_2AC_{60} salts [86]. The affinity of these compounds to polymerize depends on the interfullerene distance, which can be controlled by choosing metal A. Na_2KC_{60} polymerizes already below 310 K [87], while Na_2RbC_{60} only below around 230 K [86], and Na_2CsC_{60} does not polymerize on cooling [88]. Both the Na_2RbC_{60} and the Na_2CsC_{60} polymer can be prepared on applying pressure [89, 88]. Polymeric Na_2KC_{60} and Na_2RbC_{60} were shown to be metallic [90, 91].

Na_4C_{60} was the first fulleride polymer containing single bonds and the first one which is two dimensional and can be synthesized at ambient pressure [92]. The structure agrees with the one calculated to be the most stable for polymers, which are built from C_{60}^{4-} ions (Fig. 12c.) [81]. Polymeric Na_4C_{60} was found to be metallic [92], and transforms to an also metallic monomer phase around 500 K [56].

Li_4C_{60} is also a two dimensional polymer, but it has a bonding pattern containing both cycloadditional and single interfullerene bonds (see Fig. 12d.) [93]. This material has an insulating ground state, but is an ionic conductor due to the high mobility of the Li^+ ions above 200 K [58].

5 Conclusions

In the present paper, we have tried to show how the Jahn-Teller effect, an inherently molecular property, influences exotic solid-state phenomena as superconductivity and magnetism in fulleride salts; and how spectroscopy can amplify the effect of distortions which are minuscule at the structural level. Vibrational and electronic spectra in the solid state can unambigously prove the dynamic character of the Mott-Jahn-Teller insulating phase, as predicted by Fabrizio and Tosatti [16]. The characteristic time scale of optical spectroscopy being much shorter than that of magnetic resonance methods, it has the advantage of detecting dynamic distortions even at room temperature. Despite the existing experimental difficulties, it would be worthwile extending the scope of measurements to more fulleride salts.

Acknowledgements Financial support was provided by the Hungarian National Research Fund and the National Office for Research and Technology under grant no. NI 67842 and T 049338.

References

1. R.C. Haddon, L.E. Brus, K. Ragavachari, Chem. Phys. Lett. **125**, 459 (1986)
2. H.A. Jahn, E. Teller, Proc. Roy. London Soc. Ser. A **191**, 220 (1937)
3. C.C. Chancey, M.C.M. O'Brien, *The Jahn-Teller Effect in C_{60} and Other Icosahedral Complexes* (Princeton University Press, Princeton, 1997)
4. G. Klupp, K. Kamarás, N.M. Nemes, C.M. Brown, J. Leao, Phys. Rev. B **73**, 085415 (2006)
5. M.C.M. O'Brien, Phys. Rev. B **53**, 3775 (1996)
6. J.L. Dunn, C.A. Bates, Phys. Rev. B **52**, 5996 (1995)
7. A. Auerbach, N. Manini, T. E, Phys. Rev. B **49**, 12998 (1994)
8. A. Ceulemans, D. Beyens, L.G. Vanquickerborne, J. Am. Chem. Soc. **106**, 5824 (1984)
9. A. Ceulemans, J. Chem. Phys. **87**, 5374 (1987)
10. J.L. Dunn, unpublished
11. J.L. Dunn, Phys. Rev. B **69**, 064303 (2004)
12. S. Tomita, J.U. Andersen, E. Bonderup, P. Hvelplund, B. Liu, S.B. Nielsen, U.V. Pedersen, J. Rangama, K. Hansen, O. Echt, Phys. Rev. Lett. **94**, 053002 (2005)
13. N. Koga, K. Morokuma, Chem. Phys. Lett. **196**, 191 (1992)
14. W.H. Green, Jr., S.M. Gorun, G. Fitzgerald, P.W. Fowler, A. Ceulemans, B.C. Titeca, J. Phys. Chem. **100**, 14892 (1996)
15. J.E. Fischer, P.A. Heiney, J. Phys. Chem. Solids **54**, 1725 (1993)
16. M. Fabrizio, E. Tosatti, Phys. Rev. B **55**, 13465 (1997)
17. J.L. Dunn, J. Phys.: Condens. Matter. **17**, 5499 (2005)
18. C.A. Reed, R.D. Bolskar, Chem. Rev. **100**, 1075 (2000)
19. V. Brouet, H. Alloul, S. Garaj, L. Forró, Struct. Bonding **109**, 165 (2004)
20. D. Arcon, R. Blinc, Struct. Bonding **109**, 231 (2004)
21. P. Kupser, J.D. Steill, J. Oomens, G. Meijer, G. von Helden, Phys. Chem. Chem. Phys. **10**, 6862 (2008)
22. A. Wachowiak, R. Yamachika, K.H. Khoo, Y. Wang, M. Grobis, D.H. Lee, S.G. Louie, M.F. Crommie, Science **310**, 468 (2005)
23. B. Liu, P. Hvelplund, S.B. Nielsen, S. Tomita, Phys. Rev. Lett. **92**, 168301 (2004)
24. S. Tomita, J.U. Andersen, H. Cederquist, B. Concina, O. Echt, J.S. Forster, K. Hansen, B.A. Huber, P. Hvelplund, J. Jensen, B. Liu, B. Manil, L. Maunory, S.B. Nielsen, J. Rangama, H.T. Schmidt, H. Zettergren, J. Chem. Phys. **124**, 024310 (2006)

25. D.A. Neumann, J.R.D. Copley, D. Reznik, W.A. Kamitakahara, J.J. Rush, R.L. Paul, R.M. Lindstrom, J. Phys. Chem. Solids **54**, 1699 (1993)
26. M. Knupfer, J. Fink, J.F. Armbruster, Z. Phys. B **101**, 57 (1996)
27. M. Knupfer, J. Fink, Phys. Rev. Lett. **79**, 2714 (1997)
28. P. Jeglic, R. Blinc, T. Apih, A. Omerzu, D. Arcon, Phys. Rev. B **68**, 184422 (2003)
29. V. Brouet, H. Alloul, S. Garaj, L. Forró, Phys. Rev. B **66**, 155124 (2002)
30. T. Pichler, R. Winkler, H. Kuzmany, Phys. Rev. B **49**, 15879 (1994)
31. G. Klupp, P. Matus, D. Quintavalle, L.F. Kiss, E. Kováts, N.M. Nemes, K. Kamarás, S. Pekker, A. Jánossy, Phys. Rev. B **74**, 195402 (2006)
32. O. Gunnarson, Rev. Mod. Phys. **69**, 575 (1997)
33. L. Degiorgi, E.J. Nicol, O. Klein, G. Grüner, P. Wachter, S.M. Huang, J. Wiley, R.B. Kaner, Phys. Rev. B **49**, 7012 (1994)
34. J. Fulara, M. Jakobi, J.P. Maier, Chem. Phys. Lett. **211**, 227 (1993)
35. H. Kondo, T. Momose, T. Shida, Chem. Phys. Lett. **237**, 111 (1995)
36. D.R. Lawson, D.L. Feldheim, C.A. Foss, P.K. Dorhout, C.M. Elliott, C.R. Martin, B. Parkinson, J. Electrochem. Soc **139**, L68 (1992)
37. J. Stinchcombe, A. Pnicaud, P. Bhyrappa, P.D.W. Boyd, C.A. Reed, J. Am. Chem. Soc. **115**, 5212 (1993)
38. W.C. Wan, X. Liu, G.M. Sweeney, W.E. Broderick, J. Am. Chem. Soc. **117**, 9580 (1995)
39. P.M. Allemand, K.C. Khemani, A. Koch, F. Wudl, K. Holczer, S. Donovan, G. Gruner, J.D. Thompson, Science **253**, 301 (1991)
40. P. Launois, R. Moret, N.R. de Souza, J.A. Azamar-Barrios, A. Pénicaud, Eur. Phys. J. B **15**, 445 (2000)
41. B. Gotschy, M. Keil, H. Klos, I. Rystau, Solid State Commun. **113**, 8266 (1994)
42. V.C. Long, J.L. Musfeldt, K. Kamarás, A. Schilder, W. Schütz, Phys. Rev. B **58**, 14338 (1998)
43. W. Bietsch, J. Bao, J. Lüdecke, S. van Smaalen, Chem. Phys. Lett. **324**, 37 (2000)
44. V.C. Long, E.C. Schundler, G. B.Adams, J. B.Page, W. Bietsch, I. Bauer, Phys. Rev. B **75**, 125402 (2007)
45. M. Polomska, J.L. Sauvajol, A. Graja, A. Girard, Solid State Commun. **111**, 107 (1999)
46. T. Kawamoto, Solid State Commun. **101**, 231 (1997)
47. K. Kamarás, L. Gránásy, D.B. Tanner, L. Forró, Phys. Rev. B **52**, 11488 (1995)
48. K. Kamarás, D.B. Tanner, L. Forró, Fullerene Sci. Tech. **5**, 465 (1997)
49. S.C. Erwin, in *Buckminsterfullerenes*, ed. by w. A. Billups, M. Ciufolini (VCH, New York, 1992), p. 217
50. Y. Sun, C.A. Reed, Chem. Commun. p. 747 (1997)
51. V. Brouet, H. Alloul, S. Garaj, L. Forró, Phys. Rev. B **66**, 155122 (2002)
52. I. Lukyanchuk, N. Kirova, F. Rachdi, C. Goze, P. Molinie, M. Mehring, Phys. Rev. B **51**, 3978 (1995)
53. R.F. Kiefl, T.L. Duty, J.W. Schneider, A. Macfarlane, K. Chow, J.W. Elzey, P. Mendels, G.D. Morris, J.H. Brewer, E.J. Ansaldo, C. Niedermayer, D.R. Noakes, C.E. Stronach, B. Hitti, J.E. Fischer, Phys. Rev. Lett. **69**, 2005 (1992)
54. P.J. Benning, F. Stepniak, J.H. Weaver, Phys. Rev. B **48**, 9086 (1993)
55. Y. Iwasa, S. Watanabe, T. Kaneyasu, T. Yasuda, T. Koda, M. Nagata, N. Mizutani, J. Phys. Chem. Solids **54**, 1795 (1993)
56. G. Oszlányi, G. Baumgartner, G. Faigel, L. Gránásy, L. Forró, Phys. Rev. B **58**, 5 (1998)
57. M. Ricco, M. Belli, D. Pontiroli, M. Mazzani, T. Shiroka, D. Arcon, A. Zorko, S. Margadonna, G. Ruani, Phys. Rev. B **75**, 081401(R) (2007)
58. D. Arcon, A. Zorko, M. Mazzani, M. Belli, D. Pontiroli, M. Ricco, S. Margadonna, New Journal of Physics **10**, 033021 (2008)
59. R.M. Fleming, M. J.Rosseinsky, A.P. Ramirez, D.W. Murphy, J.C. Tully, R.C. Haddon, T. Siegrist, R. Tycko, S.H. Glarum, P. Marsh, G. Dabbagh, S.M. Zahurak, A.V. Makhija, C. Hampton, Nature **352**, 701 (1991)
60. P. Dahlke, M.J. Rosseinsky, Chem. Mater. **14**, 1285 (2002)
61. P. Dahlke, P.F. Henry, M.J. Rosseinsky, J. Mater. Chem. **8**, 1571 (1998)

62. C. Goze, F. Rachdi, M. Mehring, Phys. Rev. B **54**, 5164 (1996)
63. A. Huq, P.W. Stephens, Phys. Rev. B **74**, 075424 (2006)
64. R. Kerkoud, P. Auban-Senzier, D. Jérome, S. Brazovskii, I. Luk'yanchuk, N. Kirova, F. Rachdi, C. Goze, J. Phys. Chem. Solids **57**, 143 (1996)
65. A. Iwasiewicz-Wabnig, T. Wagberg, T.L. Makarova, B. Sundqvist, Phys. Rev. B **77**, 085434 (2008)
66. C.A. Kuntscher, G.M. Bendele, P.W. Stephens, Phys. Rev. B **55**, R3366 (1997)
67. J. Reichenbach, F. Rachdi, I. Luk'yanchuk, M. Ribet, G. Zimmer, M. Mehring, J. Chem. Phys. **101**, 4585 (1994)
68. M.G. Mitch, J.S. Lannin, Phys. Rev. B **51**, 6784 (1995)
69. Y. Iwasa, T. Kaneyasu, Phys. Rev. B **51**, 3678 (1995)
70. G. Klupp, K. Kamarás, J. Mol. Struct. **838**, 74 (2007)
71. A.J. Fowkes, J.M. Fox, P.F. Henry, S.J. Heyes, M.J. Rosseinsky, J. Am. Chem. Soc. **119**, 10413 (1997)
72. P. Paul, Z. Xie, R. Bau, P.D.W. Boyd, C.A. Reed, J. Am. Chem. Soc. **116**, 4145 (1994)
73. T. Yildirim, J.E. Fischer, P.W. Stephens, A.R. McGhie, in *Progress in Fullerene Research*, ed. by H. Kuzmany, J. Fink, M. Mehring, S. Roth (1994), p. 235
74. T. Yildirim, J.E. Fischer, A.B. Harris, P.W. Stephens, D. Liu, L. Brard, M. Strongin, A.B.S. III, Phys. Rev. Lett. **71**, 1383 (1993)
75. P. Durand, G.R. Darling, Y. Dubitsky, A. Zaopo, M.J. Rosseinsky, Nat. Matter. **2**, 605 (2003)
76. K.M. Allen, W.I.F. David, J.M. Fox, R.M. Ibberson, M.J. Rosseinsky, Chem. Mater. **7**, 764 (1995)
77. Y. Iwasa, T. Takenobu, J. Phys.: Condens. Matter **15**, R495 (2003)
78. J.E. Han, O. Gunnarsson, V.H. Crespi, Phys. Rev. Lett. **90**, 167006 (2003)
79. G. Faigel, G. Bortel, M. Tegze, L. Gránásy, S. Pekker, G. Oszlányi, O. Chauvet, G. Baumgartner, L. Forró, P.W. Stephens, G. Mihály, A. Jánossy, Phys. Rev. B **52**, 3199 (1995)
80. R.W. Schurko, M.J. Willans, B. Skadtchenko, D.M. Antonelli, J. Solid State Chem. **177**, 2255 (2004)
81. S. Pekker, G. Oszlányi, G. Faigel, Chem. Phys. Letters **282**, 435 (1998)
82. E. Kováts, G. Oszlányi, S. Pekker, J. Phys. Chem. B **109**, 11913 (2005)
83. P.W. Stephens, G. Bortel, G. Faigel, M. Tegze, A. Jánossy, S. Pekker, G. Oszlányi, L. Forró, Nature **370**, 636 (1994)
84. M.C. Martin, D. Koller, X. Du, P.W. Stephens, L. Mihaly, Phys. Rev. B **49**, 10818 (1994)
85. G. Oszlányi, G. Bortel, G. Faigel, L. Gránásy, G.M. Bendele, P.W. Stephens, L. Forró, Phys. Rev. B **54**, 11849 (1996)
86. G.M. Bendele, P.W. Stephens, K. Prassides, K. Vavekis, K. Kodatos, K. Tanigaki, Phys. Rev. Letters **80**, 736 (1998)
87. T. Saito, V. Brouet, H. Alloul, L. Forró, in *Electronic Properties of Novel Materials Molecular Nanostructures*, vol. 544, ed. by H. Kuzmany, S. Roth, M. Mehring, J. Fink (2000), vol. 544, p. 120
88. S. Margadonna, C.M. Brown, A. Lappas, K. Prassides, K. Tanigaki, K.D. Knudsen, T.L. Bihan, M. Mézouar, J. Solid State Chem. **145**, 471 (1999)
89. Q. Zhu, Phys. Rev. B **52**, R723 (1995)
90. D. Arcon, K. Prassides, S. Margadonna, A.L. Maniero, L.C. Brunel, K. Tanigaki, Phys. Rev. B **60**, 3856 (1999)
91. N. Cegar, F. Simon, G. Baumgartner, A. Sienkiewicz, L. Forró, B. Ruziska, L. Degiorgi, L. Mihály, in *Electronic Properties of Novel Materials Science and Technology of Molecular Nanostructures*, vol. 486, ed. by H. Kuzmany, S. Roth, M. Mehring (1999), vol. 486, p. 64
92. G. Oszlányi, G. Baumgartner, G. Faigel, L. Forró, Phys. Rev. Letters **78**, 4438 (1997)
93. S. Margadonna, D. Pontiroli, M. Belli, T. Shiroka, M. Ricco, M. Brunelli, J. Am. Chem. Soc. **126**, 15032 (2004)